



**Providing Choice & Value**

Generic CT and MRI Contrast Agents



**FRESENIUS  
KABI**

**CONTACT REP**

**AJNR**

**Differences in Cerebral Aneurysm Rupture  
Rate According to Arterial Anatomies  
Depend on the Hemodynamic Environment**

S. Fukuda, Y. Shimogonya and N. Yonemoto

*AJNR Am J Neuroradiol* 2019, 40 (5) 834-839

doi: <https://doi.org/10.3174/ajnr.A6030>

<http://www.ajnr.org/content/40/5/834>

This information is current as  
of July 31, 2025.

# Differences in Cerebral Aneurysm Rupture Rate According to Arterial Anatomies Depend on the Hemodynamic Environment

 S. Fukuda,  Y. Shimogonya, and  N. Yonemoto, on behalf of the CFD ABO Study Group



## ABSTRACT

**BACKGROUND AND PURPOSE:** Cerebral aneurysms have significantly different rupture rates depending on their size and location. The mechanisms underlying these differences are unclear. We examined whether anatomic rupture risks are dependent on the hemodynamic environment on the aneurysmal surface.

**MATERIALS AND METHODS:** Patient-specific geometries and flow rates of 84 cerebral aneurysms (42 anterior communicating artery and 42 MCA aneurysms) were acquired from our clinical study, the Computational Fluid Dynamics Analysis of Blood Flow in Cerebral Aneurysms: Prospective Observational Study. Pulsatile blood flow was simulated to calculate hemodynamic metrics with special attention to wall shear stress magnitude and temporal disturbance. Multivariate analyses were performed to identify associations between hemodynamic metrics and known rupture predictors (age, sex, hypertension, smoking history, location, and size).

**RESULTS:** All the wall shear stress magnitude–based metrics showed a significant negative association with size and location ( $P < .03$ ), but not other risk factors. All the wall shear stress disturbance–based metrics were significantly related to size ( $P < .001$ ). Only normalized transverse wall shear stress, a metric for multidirectional wall shear stress disturbance, was related to location ( $P = .03$ ). The normalized transverse wall shear stress had the highest odds ratio for location and size among hemodynamic metrics (odds ratios, 1.275 and 1.579; 95% confidence intervals, 1.020–1.693 and 1.238–2.219, respectively). Among the arterial geometric parameters, the aspect ratio had the second strongest association with all hemodynamic metrics, after our newly proposed aspect ratio–asphericity index.

**CONCLUSIONS:** The differences in aneurysm rupture rates according to size and location may reflect differences in hemodynamic environments in qualitatively different ways. An enhanced multidirectional wall shear stress disturbance may be especially associated with aneurysm rupture.

**ABBREVIATIONS:** AAI = aspect ratio–asphericity index; AcomA = anterior communicating artery;  $\beta$  = regression coefficient; CFD = computational fluid dynamics; GON = gradient oscillatory number; NtransWSS = normalized transverse wall shear stress; NWSS = normalized wall shear stress; NWSSG = normalized wall shear stress gradient; OSI = oscillatory shear index; TAWSS = time-averaged wall shear stress; TAWSSG = time-averaged wall shear stress gradient; WSS = wall shear stress

Cerebral aneurysm rupture is a major cause of life-threatening SAH, with high mortality and disability rates. Although sev-

eral known risk factors exist, including size, location, sex, age, history of hypertension, and smoking, it remains difficult to predict which cerebral aneurysms are more likely to rupture.<sup>1–4</sup> New predictors of cerebral aneurysm rupture are thus needed.

Aneurysm ruptures are mainly attributable to the biologic process of the progressive degradation of vessel wall structure and strength, in which hemodynamic stress and inflammation are thought to be closely involved.<sup>1,5–7</sup> We have focused on the role of hemodynamics and are using computational fluid dynamics

Received November 26, 2018; accepted after revision March 11, 2019.

From the Department of Neurosurgery (S.F.), National Hospital Organization Kyoto Medical Center, Kyoto, Japan; College of Engineering (Y.S.), Nihon University, Koriyama, Japan; and Department of Biostatistics (N.Y.), Kyoto University, Kyoto, Japan

Shunichi Fukuda and Yuji Shimogonya contributed equally to this work.

The CFD ABO Study Group Member List is in the On-line Appendix.


This work is supported by a grant-in-aid for the Japanese National Hospital Organization Multi-Center Clinical Research, AMED, under grant No. JP15gm0810006h0301, and JSPS KAKENHI grant No. 15K10323.


Paper previously presented, in part, at: International Stroke Conference 2018, January 23–25, 2018; Los Angeles, California.

Please address correspondence to Shunichi Fukuda, MD, Department of Neurosurgery, National Hospital Organization Kyoto Medical Center, 1-one Mukaihata-cho,

Fukakusa, Fushimi-ku, Kyoto City, Kyoto, Japan 612-8555; e-mail: fukudashunichi@gmail.com

 Indicates open access to non-subscribers at [www.ajnr.org](http://www.ajnr.org)

 Indicates article with supplemental on-line appendix and tables.

 Indicates article with supplemental on-line photos.

<http://dx.doi.org/10.3174/ajnr.A6030>

(CFD) techniques to clarify hemodynamics-related factors of cerebral aneurysm ruptures. We are currently conducting the Computational Fluid Dynamics Analysis of Blood Flow in Cerebral Aneurysms: Prospective Observational Study (the CFD ABO Study) as a multi-institutional prospective observational clinical study of the National Hospital Organization in Japan (UMIN000013584). Individual flow rates and arterial geometries were acquired from 461 registered patients to provide realistic patient-specific CFD models.

Among the known predictors of rupture, cerebral artery anatomic parameters such as size and location are the most significant.<sup>1–4</sup> The rupture rate of aneurysms with sizes of 7–10 mm is approximately 3 times higher than that of 3–5 mm aneurysms.<sup>2</sup> The rupture rate of anterior communicating artery (AcomA) aneurysms is approximately twice that of MCA aneurysms.<sup>2</sup> Several researchers have reported that low wall shear stress (WSS) and disturbed WSS are significantly associated with aneurysm rupture.<sup>1,6,8,9</sup> However, the relationships between these anatomic risk factors and the hemodynamic environment and the underlying mechanisms remain unclear. A better understanding of these phenomena could improve the prediction of aneurysm ruptures.

Given the above-described background, we hypothesized that rupture risks based on arterial anatomic parameters are determined by the hemodynamics—that is, the hemodynamic environment on the aneurysmal surface may vary depending on the size and location of the aneurysm, and changes in the hemodynamic environments may cause differences in the rupture-risk rate. We examined the associations between known risk factors and hemodynamic metrics on the aneurysmal surface, and we considered the mechanisms from the point of view of fluid mechanics. We applied CFD and multivariate analysis to 84 cases of bifurcation-type aneurysms located at 2 representative and frequently involved sites, the MCA and AcomA, from the CFD ABO Study. We also explored which geometry-related metrics of aneurysms (among size and 8 other known geometric parameters) were best correlated with the detected hemodynamics metrics.

## MATERIALS AND METHODS

See the On-line Appendix for details of the CFD ABO study methodology.

### Data Sources

3D-CTA images and patient-specific physiologic data, including the flow rate, were acquired from patients who consented to participate in either the CFD ABO Study approved by the National Hospital Organization, Japan, or the pilot study approved by the Ethics Committee of the Kyoto Medical Center, Japan. We analyzed 84 bifurcation-type aneurysms (42 AcomA and 42 MCA aneurysms). A flow chart of the method used is provided in On-line Fig 1.

### CFD Modeling and Postprocessing

Pulsatile blood flow was simulated using the CFD software package ANSYS CFX (ANSYS, Canonsburg, Pennsylvania). We then calculated 7 hemodynamic metrics and 9 geometric parameters during postprocessing for use in statistical analy-

## Characteristics of the cases with cerebral aneurysms<sup>a</sup>

Characteristics	
Women (No.) (%)	43 (51.2%)
Age (yr)	70.4 ± 9.0
Age 70 yr or older	46 (54.8%)
Hypertension (No.) (%)	62 (73.8%)
Smoking history (No.) (%)	49 (58.3%)
AcomA (No.) (%)	42 (50.0%)
Size (mm)	5.64 ± 2.04
Surface area (mm <sup>2</sup> )	60.0 ± 44.8
Volume (mm <sup>3</sup> )	45.5 ± 48.8
Size ratio	2.42 ± 1.08
Area ratio	14.9 ± 14.1
Aspect ratio	0.93 ± 0.39
Aspect ratio—asphericity index	0.565 ± 0.246
Parent artery diameter (mm)	2.45 ± 0.53
Aneurysm surface-averaged TAWSS (Pa)	4.68 ± 4.96
Aneurysm surface-averaged NWSS	5.88 ± 6.58
Aneurysm surface-averaged TAWSSG (Pa/mm)	5.15 ± 6.14
Aneurysm surface-averaged NWSSG	16.0 ± 19.9
Aneurysm surface-averaged OSI	0.0169 ± 0.0144
Aneurysm surface-averaged GON	0.0664 ± 0.0523
Aneurysm surface-averaged NtransWSS	0.130 ± 0.059

<sup>a</sup> Data are mean ± SD unless otherwise indicated.

ses. The CFD modeling and postprocessing details are described in the On-line Appendix.

### Statistical Analysis

The continuous data are reported as means ± SDs and were analyzed using the Wilcoxon rank sum test. A multivariate regression analysis was performed to investigate the influence of known risk factors for rupture—ie, size (the maximum diameter of the cerebral aneurysm), location (AcomA versus MCA), sex, age, history of hypertension and smoking—on the 7 hemodynamic metrics: the time-averaged wall shear stress (TAWSS), normalized WSS (NWSS), time-averaged WSS gradient (TAWSSG), normalized WSS gradient (NWSSG), oscillatory shear index (OSI), gradient oscillatory number (GON), and normalized transverse WSS (NtransWSS).

We performed a multivariate logistic analysis to determine the effects of the 7 hemodynamic metrics on size (<7 versus ≥7 mm) and location. We also performed a multivariate regression analysis to determine the associations between the known arterial geometric parameters and hemodynamic metrics after adjustment for age, sex, hypertension, smoking history, and aneurysm location. The rationales for risk-factor selection are described in the On-line Appendix. We computed regression coefficients with 95% CIs and *P* values for the models. Differences with *P* < .05 were considered significant. All analyses were performed using JMP, Version 11.0.0 software (SAS Institute, Cary, North Carolina).

## RESULTS

### Characteristics

The case characteristics are summarized in the Table.

### Association of Known Rupture Risk Factors with Hemodynamic Metrics

To investigate whether known rupture risk factors are hemodynamically involved in rupture, we examined the association be-

tween each rupture risk factor and hemodynamic metrics using a multivariate regression analysis (On-line Table 1 and On-line Fig 3). The size and WSS magnitude–based metrics, TAWSS, NWSS, TAWSSG, and NWSSG, were significantly negatively correlated, indicated by the following: TAWSS regression coefficient ( $\beta$ ),  $-0.561$  (95% CI,  $-1.064$  to  $-0.058$ )  $P = .02$ ; NWSS  $\beta$ ,  $-0.867$  (95% CI,  $-1.510$  to  $-0.224$ )  $P = .008$ ; TAWSSG  $\beta$ ,  $-0.868$  (95% CI,  $-1.486$  to  $-0.249$ )  $P = .006$ ; NWSSG  $\beta$ ,  $-3.22$  (95% CI,  $-5.16$  to  $-1.28$ )  $P = .001$ . The WSS disturbance–based metrics, OSI, GON, and NtransWSS, were significantly positively correlated as indicated by the following: OSI  $\beta$ ,  $0.00332$  (95% CI,  $0.00191$ – $0.00472$ )  $P < .001$ ; GON  $\beta$ ,  $0.0145$  (95% CI,  $0.0097$ – $0.0193$ )  $P < .001$ ; NtransWSS  $\beta$ ,  $0.0145$  (95% CI,  $0.0089$ – $0.0200$ )  $P < .001$ .

In contrast, a significant negative association was observed between the location (MCA versus AcomA aneurysms) and each of the WSS magnitude–based metrics: TAWSS  $\beta$ ,  $-1.82$  (95% CI,  $-2.84$  to  $-0.80$ )  $P < .001$ ; NWSS  $\beta$ ,  $-2.45$  (95% CI,  $-3.75$  to  $-1.15$ )  $P < .001$ ; TAWSSG  $\beta$ ,  $-2.05$  (95% CI,  $-3.31$  to  $-0.80$ )  $P = .001$ ; NWSSG  $\beta$ ,  $-6.91$  (95% CI,  $-10.84$  to  $-2.98$ )  $P < .001$ . A significant positive association with the location was found in only NtransWSS as a metric for multidirectional WSS disturbance among all of the WSS disturbance–based metrics examined ( $\beta$ ,  $0.0119$ ; 95% CI,  $0.0006$ – $0.0232$ ;  $P = .03$ ).

#### **Association of Hemodynamic Metrics with the Size and Location of Cerebral Aneurysms**

Using a multivariate logistic analysis, we sought to identify which hemodynamic metric was most strongly related to the size ( $<7$  versus  $\geq 7$  mm) and location in which significant hemodynamic involvement was observed. Although all of the hemodynamic metrics showed a significant association with both size and location, the NtransWSS had the highest OR and the strongest association with both size (OR,  $1.579$ ; 95% CI,  $1.238$ – $2.128$ ) and location (OR,  $1.275$ ; 95% CI,  $1.020$ – $1.639$ ) (On-line Table 1).

#### **Association between Aneurysm Arterial Geometric Parameters and Hemodynamic Metrics**

Several arterial geometric parameters have been reported as predictors of aneurysm rupture, such as size, size ratio, and aspect ratio. We therefore examined which arterial geometric parameter most strongly reflects each hemodynamic metric by performing a multivariate regression analysis. Among the known arterial geometric rupture risk factors, the aspect ratio showed the strongest association with all hemodynamic metrics as shown in On-line Table 2: TAWSS  $\beta$ ,  $-2.46$  (95% CI,  $-5.12$  to  $-0.21$ )  $P = .07$ ; NWSS  $\beta$ ,  $-3.20$  (95% CI,  $-6.65$  to  $0.25$ )  $P = .06$ ; TAWSSG  $\beta$ ,  $-2.92$  (95% CI,  $-6.26$  to  $-0.42$ )  $P = .08$ ; NWSSG  $\beta$ ,  $-10.5$  (95% CI,  $-21.1$  to  $-0.2$ )  $P = .05$ ; OSI  $\beta$ ,  $0.00799$  (95% CI,  $0.00017$ – $0.01616$ )  $P = .05$ ; GON  $\beta$ ,  $0.0352$  (95% CI,  $0.0057$ – $0.0648$ )  $P = .02$ ; NtransWSS  $\beta$ ,  $0.0379$  (95% CI,  $0.0052$ – $0.0707$ )  $P = .02$ .

However, the aspect ratio–asphericity index (AAI), our newly proposed geometric parameter, was more strongly correlated with all the hemodynamic metrics than the aspect ratio: TAWSS  $\beta$ ,  $-4.02$  (95% CI,  $-8.23$  to  $-0.19$ )  $P = .06$ ; NWSS  $\beta$ ,  $-5.46$  (95% CI,  $-10.90$  to  $-0.01$ )  $P = .04$ ; TAWSSG  $\beta$ ,  $-4.72$  (95% CI,  $-9.99$  to  $-0.56$ )  $P = .07$ ; NWSSG  $\beta$ ,  $-17.3$  (95% CI,  $-34.0$  to

$-0.5$ )  $P = .04$ ; OSI  $\beta$ ,  $0.0121$  (95% CI,  $0.0008$ – $0.0250$ )  $P = .06$ ; GON  $\beta$ ,  $0.0559$  (95% CI,  $0.0092$ – $0.1027$ )  $P = .01$ ; NtransWSS  $\beta$ ,  $0.0558$  (95% CI,  $0.0038$ – $0.1079$ )  $P = .03$ . Here, AAI is defined as  $(H / N) \times (d^2 / S)$ , where  $H$  is the height,  $N$  the neck width,  $d$  the size, and  $S$  the surface area.

#### **Differences in Flow Rates in Parent Vessels and Size between the AcomA and MCA Aneurysms**

The anterior cerebral artery flow rate ( $90.9 \pm 41.9$  mL/min) was significantly lower than the MCA flow rate ( $123.0 \pm 50.9$  mL/min) ( $P < .001$ ; On-line Table 3). The size was slightly, but not significantly, larger in the AcomA aneurysms ( $5.82 \pm 2.10$  mm) than the MCA aneurysms ( $5.46 \pm 2.00$  mm).

#### **Differences in Flow Rates in Parent Vessels and Size between the 2 Different Size Groups**

The parent vessel flow rate was not significantly different between the large ( $\geq 7$  mm;  $92.2 \pm 41.9$  mL/min) and small aneurysm groups ( $<7$  mm;  $112.8 \pm 50.8$  mL/min; On-line Table 4). The size was significantly greater in the large ( $8.28 \pm 1.16$  mm) than in the small ( $4.58 \pm 1.17$  mm) aneurysm group ( $P < .001$ ).

#### **Differences in Hemodynamic Metrics between Size Groups with a Threshold of 5 or 7 mm**

Using a multivariate regression analysis, we examined the differences in hemodynamic metrics between the 2 different size groups with a threshold of 5 or 7 mm (On-line Table 5). The WSS magnitude–based metrics and size were better correlated in the 5–than the 7-mm threshold ( $\beta$ , 5 versus 7 mm; TAWSS,  $-1.27$  versus  $-1.20$ ; NWSS,  $-2.37$  versus  $-1.48$ ; TAWSSG,  $-1.89$  versus  $-1.70$ ; NWSSG,  $-7.97$  versus  $-5.20$ ), whereas in the WSS disturbance–based metrics, the association was stronger in the 7–than the 5-mm threshold ( $\beta$ , 5 versus 7 mm; OSI,  $0.00367$  versus  $0.00648$ ; GON,  $0.0207$  versus  $0.0260$ ; NtransWSS,  $0.0176$  versus  $0.0274$ ).

#### **Flow Rates and TAWSS on the ICA in MCA Aneurysm Cases**

In the MCA aneurysm cases, both the flow rate and the TAWSS on the ICA on the side where the aneurysm was present were significantly higher in the large ( $\geq 5$  mm) than the small ( $<5$  mm) aneurysm group ( $P = .03$  and  $.03$ , respectively; On-line Table 6).

### **DISCUSSION**

Hemodynamics is likely involved in cerebral aneurysm ruptures, and some of the rupture predictors become significant risk factors due to the influence of hemodynamics.<sup>1,5–7</sup> Several studies have quantitatively examined hemodynamic metrics in ruptured and unruptured cerebral aneurysms.<sup>7,10</sup> These reports examined the degree of association between hemodynamic metrics and aneurysm rupture and demonstrated that ruptured and unruptured aneurysms had significantly different hemodynamic characteristics.<sup>10</sup> Therefore, it is presumed that some of the known rupture risks become significant by reflecting the influence of these hemodynamic environments. However, to our knowledge, no report has described the significance of the association between hemodynamic parameters as independent variables and the rupture risks, such as size and location, or conversely, how much the rup-



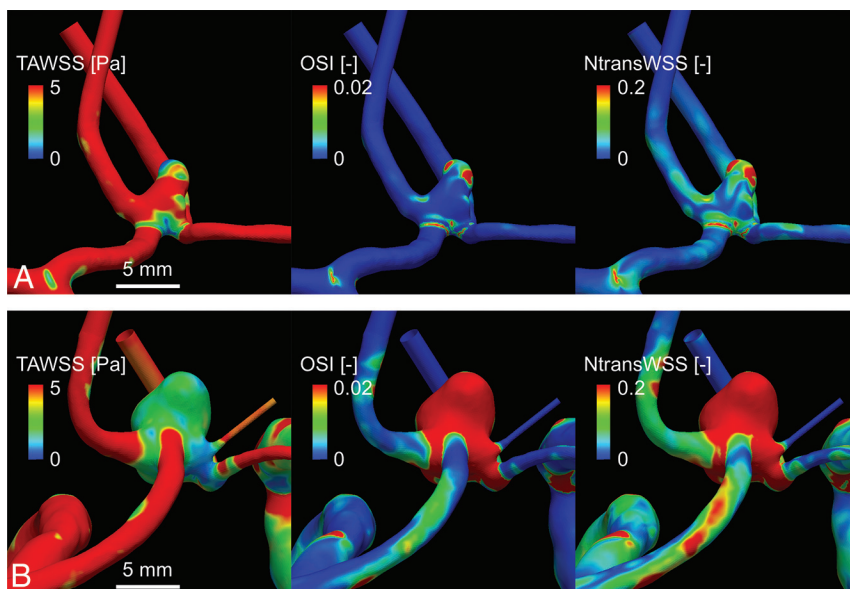


**FIG 1.** Comparisons of hemodynamic metrics between a representative small aneurysm (A) and a large aneurysm (B).

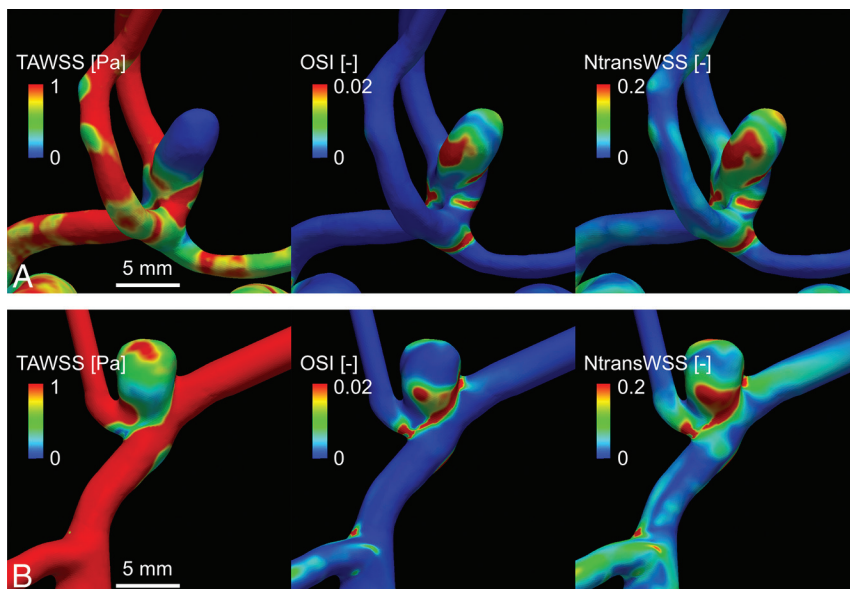


**FIG 2.** Comparisons of hemodynamic metrics between a representative anterior communicating artery aneurysm (A) and an MCA aneurysm (B).

ture risks as independent variables are related to hemodynamic environments, though several reports have examined the association between hemodynamic factors and rupture itself.<sup>7,10</sup> Therefore, we statistically examined the mutual relationship between hemodynamic parameters and representative risk factors such as age, sex, smoking history, and hypertension in addition to size and location. This is thus the first examination of this type. The results of our analyses indicate that arterial anatomic parameters (size and location of aneurysms) and hemodynamic metrics characterizing the WSS magnitude and disturbance were significantly associated; both the associations of the arterial anatomic parameters with the hemodynamic metrics and the associations of the hemodynamic metrics with the arterial anatomic parameters were statistically significant (On-line Table 1 and On-line Fig 3), sug-

gesting that rupture risks based on arterial anatomic parameters are determined by the hemodynamic environment.

Larger and AcomA aneurysms have higher rupture rates than smaller and MCA aneurysms, respectively.<sup>2</sup> The present results show that the TAWSS on the aneurysmal surface was significantly negatively associated with size and location (On-line Table 1 and Figs 1 and 2 and On-line Figs 3–5). This finding is consistent with studies showing that a significant decrease in the magnitude of the WSS on the aneurysmal surface is closely associated with the aneurysm rupture status.<sup>1,6,8,9</sup>

This leads us to ask what mechanisms cause the WSS to become low or disturbed depending on the size and location. Are the mechanisms different between size and location? Based on the present data, we considered the mechanisms from the point of view of fluid mechanics. The finding that the TAWSS was significantly decreased on AcomA aneurysms compared with MCA aneurysms could be explained qualitatively. It is hemodynamically clear that the TAWSS on the aneurysmal surface is affected principally by the size of the aneurysm and the inflow rate into the aneurysm.<sup>11</sup> The larger the size of the aneurysm (ie, the larger the open space inside the aneurysm) and the lower the inflow rate, the lower the TAWSS will be.

Because it was difficult to measure the inflow rate into the aneurysm for all the cases, we use the flow rate in the parent vessel, the anterior cerebral artery or MCA, in the following discussion. In our results, the anterior cerebral artery flow rate was significantly lower than the MCA flow rate, whereas the aneurysmal size showed no significant difference between the AcomA and MCA aneurysm

groups (On-line Table 3). Therefore, the significant difference in TAWSS between the 2 groups was due mainly to the difference in flow rates. In contrast, the decrease in the TAWSS with increasing aneurysm size may be explained simply by the effect of size because the flow rate in the parent vessel showed no difference between the 2 size groups (On-line Table 4).

A significant positive association was observed between each of the WSS disturbance-based metrics (the OSI, GON, and NtransWSS) and the size of the aneurysm (On-line Table 1, Fig 1, and On-line Fig 4). With respect to location, however, only NtransWSS differed significantly among the different locations (On-line Table 1, Fig 2, and On-line Fig 5). These findings suggest that aneurysm size and location both contribute significantly to

the hemodynamic disturbance, but in qualitatively different ways. In the present study, we defined a new metric, the NtransWSS, by dividing the nodal transverse WSS<sup>12</sup> by the TAWSS at the same node because this normalization allowed us to compare the transverse WSS among multiple cases on the same basis. The OSI can distinguish between purely forward (low OSI) and reversing unidirectional (high OSI) flow, but the NtransWSS cannot (low NtransWSS in both cases). In contrast, the NtransWSS can distinguish between reversing unidirectional (low NtransWSS) and multidirectional (high NtransWSS) flow, but the OSI cannot (high OSI in both cases).<sup>12</sup>

It thus seems reasonable to infer that the hemodynamic environments of small and large aneurysms are characterized in part by purely forward and multidirectional WSS, respectively, because both the OSI and NtransWSS were significantly different. In contrast, the hemodynamic environment of the MCA and AcomA aneurysms may be characterized in part by reversing unidirectional and multidirectional WSS, respectively, because significant variations were observed in the NtransWSS, but not in the OSI. The more disturbed hemodynamic stress at AcomA aneurysms compared with MCA aneurysms may be because AcomA, but not MCA, aneurysms are positioned along the circle of Willis.

Among the hemodynamic metrics, the NtransWSS had the highest OR for both size and location (On-line Table 1). This suggests that rupture rates in aneurysms of different sizes and locations are most strongly influenced by the multidirectional disturbance in WSS. Several experimental studies have reported that low WSS or disturbed WSS without a clear direction, ie, multidirectional WSS, or both cause sustained molecular signaling of proinflammatory and proliferative pathways of vascular endothelial cells.<sup>13,14</sup> The inflammatory processes in vessel walls play a critical role in the pathogenesis of cerebral aneurysms.<sup>15–17</sup> Therefore, the clinical evidence of higher rupture rates in AcomA aneurysms and larger aneurysms might be associated, in part, with the inflammation in the vessel walls enhanced by the low WSS and the multidirectionally disturbed WSS detected by the NtransWSS.<sup>7,18</sup>

Several researchers have proposed various aneurysmal geometric parameters for predicting rupture risk.<sup>19–21</sup> The use of surrogate geometric parameters of the hemodynamic environment with high rupture risk would be of great clinical value because geometric parameters can be measured more easily than hemodynamic metrics at clinical sites. We thus investigated which previously proposed geometric parameters of aneurysms best correlated with the TAWSS and NtransWSS. Our analyses revealed that the aspect ratio was most strongly correlated with both the TAWSS and NtransWSS, followed by the size ratio. The aspect ratio has been reported to play a greater role than the size in the rupture of AcomA and MCA aneurysms.<sup>19,20</sup> The size ratio has been reported to be a useful rupture risk predictor, particularly for small aneurysms of <5 mm.<sup>21</sup>

However, the correlation between some geometric parameters, including size ratio and aspect ratio, and aneurysm rupture is still controversial.<sup>22</sup> This is presumably because these geometric parameters only partially reflect hemodynamic environments (On-line Table 2). Therefore, we defined a novel geometric parameter, the AAI, which serves as a special refined geometric marker for the nonsphericity of aneurysmal shapes.

The AAI best reflected both the TAWSS and the NtransWSS among all of the geometric parameters examined (On-line Table 2). The AAI is thus a potentially useful geometric parameter for predicting the rupture risk of aneurysms. We will validate its usefulness on completion of the ABO study. Because CFD analyses currently take time and effort, it is clinically impractical to conduct them for all unruptured aneurysm cases. Thus, the use of arterial geometric parameters may be more convenient at the clinical level. Indeed, it might be reasonable to first perform a screening with useful arterial geometric parameters and then to examine the detailed hemodynamics using a CFD analysis for essential cases.

To better understand how the hemodynamic metrics change with increasing aneurysm size, we examined the threshold size at which the hemodynamic metrics changed notably. The difference in the WSS magnitude–based metrics between the 2 different size groups with a threshold of 5 mm was larger than that with a threshold of 7 mm, whereas the difference in the WSS disturbance–based metrics between the 2 different size groups with a threshold of 7 mm was larger than that when the threshold was 5 mm (On-line Table 6). In other words, as the aneurysm size increases, the magnitude of the WSS declines first, and then the WSS disturbance occurs. Cerebral aneurysms may have at least 2 different critical sizes at which the rupture risk is heightened.

In the CFD ABO study, individual flow rates and arterial geometries have been acquired from each registered patient to provide realistic patient-specific CFD models. In most hemodynamic cohort studies using CFD analyses, the inlet boundary conditions are based on a typical flow velocity or flow rate of healthy subjects.<sup>7,18</sup> Alternatively, in other studies, the inlet boundary conditions were set so that the mean WSS at the ICA was equal to 1.5 Pa.<sup>23</sup> However, we found that the mean flow rate and the WSS at the ICA of the large MCA cases ( $\geq 5$  mm) were significantly higher than those of the small MCA cases ( $< 5$  mm; On-line Table 6). Thus, the mean WSS at the ICA is not constant but strongly depends on characteristics of the individual case. Because such substantial differences are thought to have a non-negligible impact on hemodynamic characteristics,<sup>10</sup> it is essential to use patient-specific inflow boundary conditions in combination with patient-specific arterial geometry in these types of statistical analyses.

The present study has some limitations. First, we did not directly measure the rupture risk, but we measured recognized risk factors for rupture. Second, it remains unclear whether the NtransWSS can further help to stratify the rupture risk of aneurysms with similar sizes and locations, though the results suggest that an enhanced NtransWSS may be strongly associated with aneurysm rupture. Third, we cannot conclude that the NtransWSS is superior to other hemodynamic metrics in terms of the risk assessment of aneurysm rupture. Fourth, only AcomA and MCA aneurysms were examined. It is unclear how the present results would change if aneurysms at other locations were included. These limitations may be resolved by a statistical hemodynamic comparison between unruptured and ruptured/enlarged aneurysms at various locations, which will be made in our ongoing clinical study.

## CONCLUSIONS

In the analysis of AcomA and MCA aneurysms, the arterial anatomic parameters (size and location) and hemodynamic metrics characterizing the WSS magnitude and disturbance were significantly associated. Therefore, the differences in the rupture rate of aneurysms for various arterial anatomic parameters may reflect the differences in the hemodynamic environment. Our results also suggest that a CFD analysis is a useful simulation that matches epidemiologic data. Although both low WSS and enhanced disturbed flow may be involved in aneurysm ruptures, an enhanced disturbance of multidirectional WSS may be most strongly associated with aneurysm ruptures; the NtransWSS, a refined hemodynamic metric proposed in the present study, had the highest OR for size and location among all the examined hemodynamic metrics including OSI. Size and location had significant effects on the hemodynamic environment in qualitatively different ways; thus, the decrease in the WSS with increasing aneurysm size may be explained by the effect of size itself, whereas the significant difference in the WSS according to location may be due to the difference in the flow rate of the parent artery. Our novel geometric parameter, the AAI, may be useful for predicting the rupture risk of aneurysms.

## ACKNOWLEDGMENTS

We thank Dr Geert W. Schmid-Schönbein, Chair of the Department of Bioengineering, University of California, San Diego, for his valuable advice. We also thank Mr Yasuhide Imoto for his assistance.

Disclosures: Shunichi Fukuda—RELATED: Grant: grant-in-aid from the Japanese National Hospital Organization Multi-Center Clinical Research, AMED, and a JSPS KAKENHI grant; Comments: This study was supported by a grant-in-aid from the Japanese National Hospital Organization Multi-Center Clinical Research, AMED, under grant No. JP15gm0810006h0301 and a JSPS KAKENHI grant No. 15K10323.

## REFERENCES

1. Etminan N, Rinkel GJ. **Unruptured intracranial aneurysms: development, rupture and preventive management.** *Nat Rev Neurol* 2016; 12:699–713 CrossRef Medline
2. Morita A, Kirino T, Hashi K, et al; the UCAS Japan Investigators. **The natural course of unruptured cerebral aneurysms in a Japanese cohort.** *N Engl J Med* 2012;366:2474–82 CrossRef Medline
3. Greving JP, Wermer M, Brown RD Jr, et al. **Development of the PHASES score for prediction of risk of rupture of intracranial aneurysms: a pooled analysis of six prospective cohort studies.** *Lancet Neurol* 2014;13:59–66 CrossRef Medline
4. Cebal JR, Raschi M. **Suggested connections between risk factors of intracranial aneurysms: a review.** *Ann Biomed Eng* 2013;41:1366–83 CrossRef Medline
5. Kayembe KN, Sasahara M, Hazama F. **Cerebral aneurysms and variations in the circle of Willis.** *Stroke* 1984;15:846–50 CrossRef Medline
6. Shimogonya Y, Fukuda S. **Computational and experimental studies into the hemodynamics of cerebral aneurysms.** *Journal of Biomechanical Science and Engineering* 2016;11:15–00488 CrossRef
7. Xiang J, Natarajan SK, Tremmel M, et al. **Hemodynamic-morphologic discriminants for intracranial aneurysm rupture.** *Stroke* 2011; 42:144–52 CrossRef Medline
8. Signorelli F, Sela S, Gesualdo L, et al. **Hemodynamic stress, inflammation, and intracranial aneurysm development and rupture: a systematic review.** *World Neurosurg* 2018;115:234–44 CrossRef Medline
9. Takao H, Murayama Y, Otsuka S, et al. **Hemodynamic differences between unruptured and ruptured intracranial aneurysms during observation.** *Stroke* 2012;43:1436–39 CrossRef Medline
10. Cebal JR, Mut F, Weir J, et al. **Quantitative characterization of the hemodynamic environment in ruptured and unruptured brain aneurysms.** *AJNR Am J Neuroradiol* 2011;32:145–51 CrossRef Medline
11. Jansen IG, Schneiders JJ, Potters WV, et al. **Generalized versus patient-specific inflow boundary conditions in computational fluid dynamics simulations of cerebral aneurysmal hemodynamics.** *AJNR Am J Neuroradiol* 2014;35:1543–48 CrossRef Medline
12. Peiffer V, Sherwin SJ, Weinberg PD. **Computation in the rabbit aorta of a new metric: the transverse wall shear stress—to quantify the multidirectional character of disturbed blood flow.** *J Biomech* 2013; 46:2651–58 CrossRef Medline
13. Aoki T, Yamamoto K, Fukuda M, et al. **Sustained expression of MCP-1 under low wall shear stress concomitant with turbulent flow in endothelial cells of intracranial aneurysm.** *Acta Neuropathol Commun* 2016;4:48 CrossRef Medline
14. Chien S. **Effects of disturbed flow on endothelial cells.** *Ann Biomed Eng* 2008;36:554–62 CrossRef Medline
15. Aoki T, Kataoka H, Shimamura M, et al. **NF- $\kappa$ B is a key mediator of cerebral aneurysm formation.** *Circulation* 2007;116:2830–40 CrossRef Medline
16. Nuki Y, Tsou TL, Kurihara C, et al. **Elastase-induced intracranial aneurysms in hypertensive mice.** *Hypertension* 2009;54:1337–44 CrossRef Medline
17. Aoki T, Fukuda M, Nishimura M, et al. **Critical role of TNF- $\alpha$ -TNFR1 signaling in intracranial aneurysm formation.** *Acta Neuropathol Commun* 2014;2:34 CrossRef Medline
18. Shojima M, Oshima M, Takagi K, et al. **Magnitude and role of wall shear stress on cerebral aneurysm: computational fluid dynamic study of 20 middle cerebral artery aneurysms.** *Stroke* 2004;35: 2500–05 CrossRef Medline
19. Lin N, Ho A, Gross BA, et al. **Differences in simple morphological variables in ruptured and unruptured middle cerebral artery aneurysms.** *J Neurosurg* 2012;117:913–19 CrossRef Medline
20. Maiti TK, Bir SC, Patra DP, et al. **158 Morphological parameters for anterior communicating artery aneurysm rupture risk assessment.** *Neurosurgery* 2016;63:163–64 CrossRef
21. Kashiwazaki D, Kuroda S; Sapporo SAH Study Group. **Size ratio can highly predict rupture risk in intracranial small (<5 mm) aneurysms.** *Stroke* 2013;44:2169–73 CrossRef Medline
22. Lauric A, Baharoglu MI, Gao BL, et al. **Incremental contribution of size ratio as a discriminant for rupture status in cerebral aneurysms: comparison with size, height, and vessel diameter.** *Neurosurgery* 2012; 70:944–51; discussion 951–52 CrossRef Medline
23. Sugiyama S, Niizuma K, Sato K, et al. **Blood flow into basilar tip aneurysms: a predictor for recanalization after coil embolization.** *Stroke* 2016;47:2541–47 CrossRef Medline